S1 Materials and Methods

S1.1 Epidemiological data and characters for this study

All reported HFMD cases from 1 January 2011 to 31 December 2019 in Guangdong and Shandong province were obtained from the National Notifiable Disease Surveillance System (NNDSS) of the Chinese Center for Disease Control and Prevention (Chinese CDC). The data included the number of weekly and monthly reported HFMD cases per city. The diagnostic criteria of HFMD were based on the diagnosis and treatment guidelines established by the National Health and Family Planning Commission of the People's Republic of China in 2018, with or without fever, vesicular rash on the hands, feet, mouth and occasionally the buttocks.

S1.1.1 Description of epidemiological data of Guangdong Province Symptomatic HFMD cases (*n* = 3,257,285) were reported in Guangdong, and the incidence of HFMD exceeded 3,000 cases per million person-years, which was more than three times the national average. Among these cases, 3,758 (0.12%) cases were confirmed as severe cases, and 179 cases were fatal cases (case fatality rate: 0.55 ‰), with a severe case fatality rate of 4.76%. There were two peaks in an epidemiology year: a summer peak was observed in May and June (Figure 2B, E-F), with a second smaller peak in October and November except for 2017, when the autumn peak that appeared in October happened to exceed the summer peak. High-risk areas of HFMD in Guangdong were located in the Pearl River Delta region, especially Zhuhai and Guangzhou, which had the highest incidence rate and reported cases in these 9 years, respectively.

S1.1.2 Description of epidemiological data of Shandong Province In Shandong Province, a total of 832,065 HFMD cases were reported, of which 5,746 (0.69%) cases developed severe complications, and 30 cases had a fatal outcome (case-fatality rate: 0.36 ‰), with a severe case-fatality rate of 0.52%. The incidence rates of HFMD cases were approximately 900–1,000 cases per million person-years in Shandong over nine years. The incidence of HFMD showed a typical major peak each year, and the reported cases began to increase in March and reached a peak from May to July (Figure 2A, C–D). High-risk areas of HFMD in Shandong were located in the provincial capital and northwest region, while the highest average incidence rate was found in Dongying on the northern coast of Shandong.

S1.2 Methods for calculation and Evaluation

S1.2.1 Spatiotemporal convolution block Through the analysis, HFMD has a high correlation in time and space, and CNN and GCN are also widely used to extract temporal and spatial characteristics of the spatiotemporal network. In this paper, spatiotemporal convolution blocks are used to extract spatiotemporal features, including two temporal convolution layers and spatial convolution layers, which are used to learn the temporal and spatial correlations respectively. The time convolution layer is processed by 1-D convolution neural network on time series, and the size of convolution kernel is k_{t}. In order to enhance the model to capture the hidden nonlinear characteristics, we introduce a gating mechanism into the time convolution layer. Assuming that the input of the model is $X \in R^{n \times T \times C_{in}}$, where n represents the number of cities, T represents the time length.C_{in} is often used to represent the input dimension of the model in deep learning methods, and it is the number of cases in each city in this model. The influence of the historical time series on the current time length is captured through the one-dimensional convolution kernel $\Gamma \in R^{1 \times K_t \times C_{in} \times 2C_{out}}$of length k_{t}. Because the convolution operation is not filled, the length of the time series will be reduced by k_{t}-1, and the output is $[Y_1, Y_2] \in R^{n \times (T-K_t+1) \times (2C_{out})}$, where Y_1, Y_2has the same dimension $Y \in R^{n \times (T-K_t+1) \times C_{out}}$, Y_1, Y_2 and X through the gating mechanism to get the final output Z.

$$Z = tconv(X)$$

$$tonv(X) = \Gamma \times_{\tau} X$$

$$\Gamma \times_{\tau} X = (X \times Y_1 + b) \odot \sigma(X \times Y_2 + c)$$

After that, the output Z of the temporal convolutional layer is sent to the spatial convolutional layer to capture the spatial structure mode. Generally speaking, graph convolution uses the method of spectral graph convolution to extend the convolution operation to graph structure data. For the graph G = (V, E), its Laplacian matrix is defined as L = D-A, and its normalized form is $\mathbf{L} = \mathbf{I}_n - \mathbf{D}^{-\frac{1}{2}}\mathbf{A}\mathbf{D}^{-\frac{1}{2}}$, where A is the adjacency matrix, $\mathbf{I}_n$ is the identity matrix, and D is the degree matrix, that is, $D_{ij} = \sum_j A_{ij}$. Since L is a symmetric matrix in this article, we use a symmetric normalized Laplacian matrix, and L can be decomposed into $L = U\Lambda U^T$

Where U is the eigenvector matrix and is the diagonal matrix of eigenvalues. However, when the graph has a large number of vertices, the calculation complexity of directly performing Eigen decomposition on the Laplacian matrix is too large. Therefore, this paper adopts the K-order Chebyshev polynomial to approximate the feature to solve the feature, so the formula for graph convolution is:

$$H = gconv(Z) = g_{\vartheta}(L)Z$$

$$g_{\vartheta}(L)Z = g_{\vartheta}\left(U\Lambda U^T\right)Z = Ug_{\vartheta}(\Lambda)U^TZ$$

$$L = I_m - D^{-\frac{1}{2}}AD^{\frac{1}{2}} = U\Lambda U^T$$

Where $T_k(\tilde{\mathbf{L}}) \in R^{n\times n}$ is the Chebyshev polynomial, k is the order of the Chebyshev polynomial, which determines the range of the convolution receptive field, $\tilde{\mathbf{L}} = \frac{2\mathbf{L}}{\lambda_{\max}} - \mathbf{I}_n$ scales the Laplacian matrix to between [-1,1], and $\lambda_{\max}$ is the largest feature of L Value, also called the spectral radius, $\vartheta_i \in R^K$ is the coefficient of the Chebyshev polynomial. By using this method, the information of the neighbor nodes of order 0~k-1 of each node is extracted to update the characteristic information of the node itself.

$$H = gonv(Z) = g_{\vartheta}(L)Z \approx \sum_{k=0}^{K-1} \vartheta_k T_k(\tilde{L})Z$$

$$\tilde{\mathbf{L}} = \frac{2\mathbf{L}}{\lambda_{\max}} - \mathbf{I}_n$$

After spectral convolution processing, the output of spatial convolution layer is put into the next layer of time convolution layer, so as to achieve further time feature extraction and obtain the complete output $X' \in R^{n\times(T-2(K_t-1))\times C'_{out}}$ of spatiotemporal convolution block. The complete processing process of spatiotemporal convolution block is as follows

$$X' = tconv(gonv(tconv(X)))$$

S1.2.2 Output layer Since the spatio-temporal convolution block has two one-dimensional convolution processes, the length of the data in the time dimension will be reduced by 2(k_t-1) every time a spatio-temporal convolution block is passed, so after two spatio-temporal convolution blocks, the output is $Y \in R^{n\times 4(T-K_t+1)\times C_{out}}$. The output layer includes two time convolutional layers and a fully connected layer, which maps the output to $Z \in R^{n\times C_o}$, the fully connected layer is $\hat{y} = Z\omega + b$, where $\in R^{C_o\times F}$ (where w is the parameter matrix and F is the number of output features), then $\hat{y} \in R^n$ is output.

S1.2.3 Evaluation about model parameters The deviation between the observed value and true value was displayed with Root Mean Square Error (RMSE) and Mean Absolute Error (MAE).

$$\mathrm{MAE} = \frac{1}{n}\sum_{t=1}^{n}\left|\{\hat{Y}_t - Y_t\}\right|$$

$$\mathrm{RMSE} = \sqrt{\frac{\sum_{t=1}^{n}\left(\hat{Y}_t - Y_t\right)^2}{n}}$$

$\hat{Y}_t, Y_t \in R^{N*T}$ was ground true data and system prediction data, respectively. For MAE and RMSE, lower value is better.

S1.2.4 Goodness of fit between the predicted curve and the actual incidence curve. The consistency between true value and predicted value was verified by R^2, and the correlation between average disease data of 2011-2018 and the predicted curve was also compared.

$$R^2 = 1 - \frac{SS_{\mathrm{Regression}}}{\mathrm{SS}_{\mathrm{Total}}} = 1 - \frac{\sum(y - \hat{y})^2}{\sum(y - \bar{y})^2}$$

$SS_{\mathrm{Regression}}$ represents the Sum Squared Regression Error, which was the distance between the true data points and the regression line square that to get squared error. SS_{Total} was the Sum Squared Total Error, which was the square error that distance between the true data dots and the mean value. Normally, R^2 is a measure of the degree of the regression model. In general, R^2 ranges from minus infinity to 1, and smaller R^2 means worse fit.

S1.2.1.5 Experimental settings Our experimental environment setup is Intel Core i5-8400 and Nvidia 970 GPU. We use an adaptive learning rateand Nvidia 970 GPU. We use an adaptive learning rate optimizer with an initial learning rate set to 0.0001. For all data, we divide them into a training set, a validation set, and a test set. We set the windows to[12,24,36] respectively. To make AR and VAR perform better, we use L2 regularization during training. For the nonlinear method, we use different numbers of hidden units to make the nonlinear model achieve better results. The probability of random inactivation in the convolution module is set to 0.5, and the training and test sets do not include missing data.

S2 Supplementary Text

S2.1 Description and verification of model parameter

S2.1.1 The effect of forecast time on forecast perfomance In order to show the influence of the prediction time on the spatial prediction effect, we selected the 29th week of Shandong Province and 25th week of Guangdong Province as the detection objects, and compared the real spatial distribution with the spatial distribution of different prediction lengths (shown in Supplementary Figure S7).

In Shandong Province (Supplementary Figure S7A), it can be found that when the predicted length is 4 weeks, the model is more inclined to spread to the periphery in the red area with severe epidemic, especially the neighboring prefecture-level cities, while the predicted length is 8 weeks and 12 weeks, with the increase in the length of the prediction period, the model decayed in the range of the ability to spread, but still captured the two serious outbreaks. In Guangdong Province (Supplementary Figure S7B), it can be clearly found that the epidemic gathering area is mainly concentrated in Pearl River Delta region. Under the predicted length of 4 weeks, the model still believes that there is a sign of proliferation in the high-incidence area and is going northwest offset, and after the prediction length is 8 weeks and 12 weeks, the model is basically consistent with the real situation, maintaining a good spatial prediction effect.

S2.1.2 The influence of historical data length on model prediction In order to better explain the impact of the length of the historical morbidity considered by the model on the prediction results, we set different parameters H. The deviation between the observed value and true value was displayed with Root Mean Square Error (RMSE) and Mean Square Error (MAE), and the results are shown in Table 1.

In Shandong Province, it can be seen that the minimum indicators were all obtained at the time of H = 24. When we define H=12h, most of the time evaluation indexes are relatively poor, which shows that less historical data is not conducive to the training of the model. Correspondingly, the error index was improved by adding the history data to 36 weeks. However, compared with H = 24, the error index was larger, which indicates that when the historical data is too large, some interference information may be added, which will affect the judgment of the model

In Guangdong Province, it can be seen that when H = 36, most of the indicators will be less effective than H = 24 and 12, which means that in this area where the incidence has two peaks a year, the model considers that history too long data time may bring too much interference information to the model, thereby increasing the prediction error of the model. When H = 12, the indicator of MAE is only slightly better than H = 24 in the fourth week, while the gap in RMSE is larger on the top. In the eighth week, the RMSE is only slightly better than when H = 24, but it is obviously worse on the MAE, and the indicators on the twelfth week are mutually advantageous.

S2.1.3 The influence of data channel size on model prediction The channel size is used to determine the number of convolution kernels in each convolution layer, and different convolution kernels are used to extract different features from the data. We can find that all the optimal parameters were pointed to channel size of (1, 4, 8) in Shandong. However, long prediction period (8 weeks and 12 weeks) were apt to the channel size of (1, 3, 1) in Guangdong, while channel size properly increased (1, 3, 6) when the prediction period was 4 weeks.

The training parameters of the model will increase rapidly when the channel number was too large, which means that the learning difficulty will be increased under the condition of the same amount of data. The high RMSE in the experimental results also proves this point. On the other hand, when the number of channels is too small, the model cannot capture the hidden features well because of the nonlinear characteristics of the disease curve in time and too few training parameters, which leads to large errors in prediction.

S2.1.4 The influence of time convolution kernel size and neighborhood number on model prediction The size of the temporal convolution kernel is very important for capturing the temporal features, and this parameter determines the size of the receptive field in each extraction process in the temporal dimension. We set the size of convolution kernel kt = 3 and kt = 5 respectively for comparative experiments. We can find that when H = 4 and 8, the index difference between the two convolution kernels is not particularly obvious, but when H = 12, the index of kt = 5 is better than kt = 3, which shows that the large convolution kernel has the advantage of larger receptive field in long-term prediction. We can get more information on the trend of time, which has a greater advantage for hand-foot-mouth disease, a disease with a longer duration.

Spatial information fusion of infectious diseases has always been a difficult point in the construction of prediction model, and how to set the fusion range of spatial information is also a matter worth discussing. Too small a range cannot fully consider the incidence of surrounding cities, and too large a range will lead to excessive smoothing of the incidence information of surrounding cities. Therefore, it is necessary to select the appropriate ks size for the establishment of the model. After many rounds of comparative test analysis, we get the conclusion that it is more appropriate to consider a city that can be reached by Ks = 4 (Shandong) and ks = 5 (Guangdong) in space, which is the space scope that the city needs to consider (Supplementary Table S3). When ks = 1, 2 and 3, the overall evaluation indexes tend to be consistent, which shows that the spatial information fusion degree is too small at this time, and the model cannot obtain enough spatial information.

S2.1.5 The influence of graph convolution module Due to the migration and flow of population, the infection of diseases usually has certain regional characteristics, so it is of great reference value to consider the incidence of diseases in neighboring cities. The prediction of the incidence of each city will be combined with the characteristics of other cities in a period of time, and the graph convolution module of spatial dimension is used to effectively capture the spatial correlation. In order to prove the effectiveness of the module, we remove the graph convolution module in the model for ablation experiments. The results are as follows. Through comparison, we can see that both MAE and RMSE have higher evaluation index than the model with graph convolution module, which shows that the model with graph convolution has certain promotion effect, because the spatial model can fully combine the incidence of the surrounding cities for prediction. The epidemic situation of infectious diseases is non-stationary in time and space, and the spatiotemporal model can reflect this feature to a certain extent, so as to obtain better prediction results.

We arranged the degree of fitting between the predicted curve and the actual incidence curve of each city in reverse order, and analyzed the average number of HFMD cases and the average incidence of HFMD in each city from 2011 to 2018.

S2.2 STGCN Model Results

S2.2.1 Predictive epidemical curve of HFMD based on the STGCN model in 2019.
S2.2.1.1 Predictive epidemical curve of Guangdong (city level)
S2.2.1.2 Predictive epidemical curve of Shandong (city level)
S2.2.2 Geospatial maps based on the STGCN model in 2019.
S2.2.2.1 Geospatial maps of Guangdong (mp4)
S2.2.2.2 Predictive epidemical curve of Shandong (mp4)

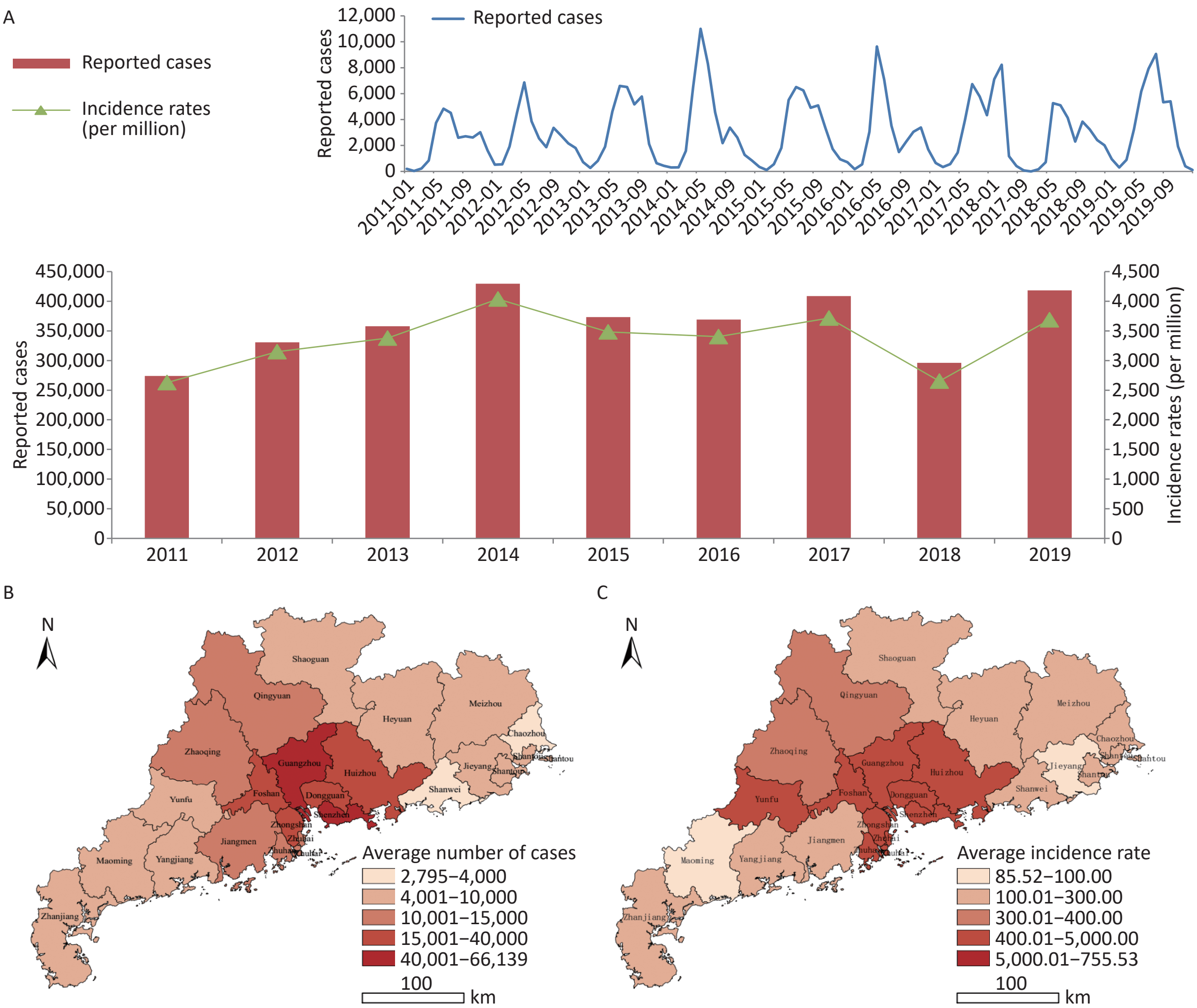

Supplementary Figure S1. (A) Epidemical curve of reported cases with HFMD between 2011 and 2019 in Guangdong. (B) Geographic distribution of average number of probable and laboratory-confirmed cases. (C) Geographic distribution of average incidence rates of probable and laboratory-confirmed cases.

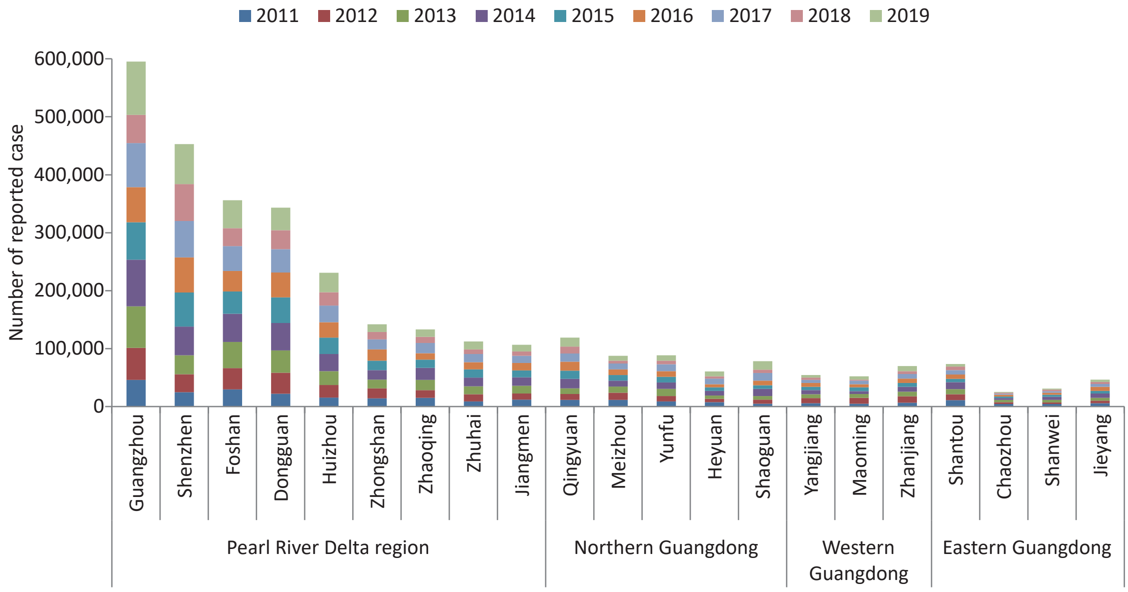

Supplementary Figure S2. Number of reported case of HFMD in cities of Guangdong province between 2011 and 2019. Data was available from Chinese Disease Prevention and Control Information System (http://10.249.1.170:81).

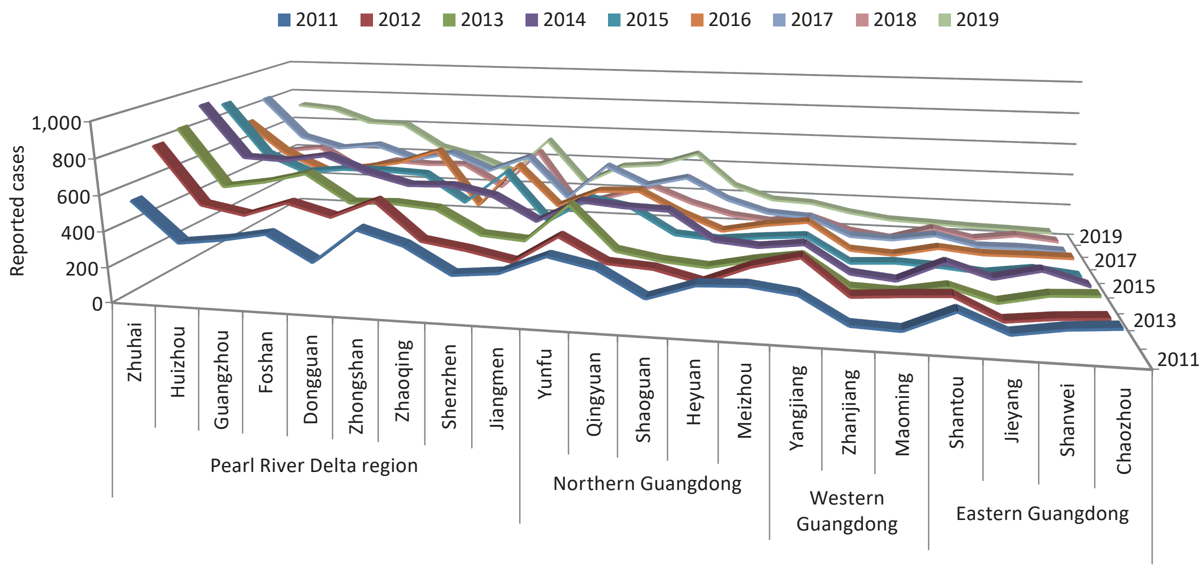

Supplementary Figure S3. Incidence of HFMD in cities of Guangdong province between 2011 and 2019. Data was available from Chinese Disease Prevention and Control Information System (http://10.249.1.170:81).

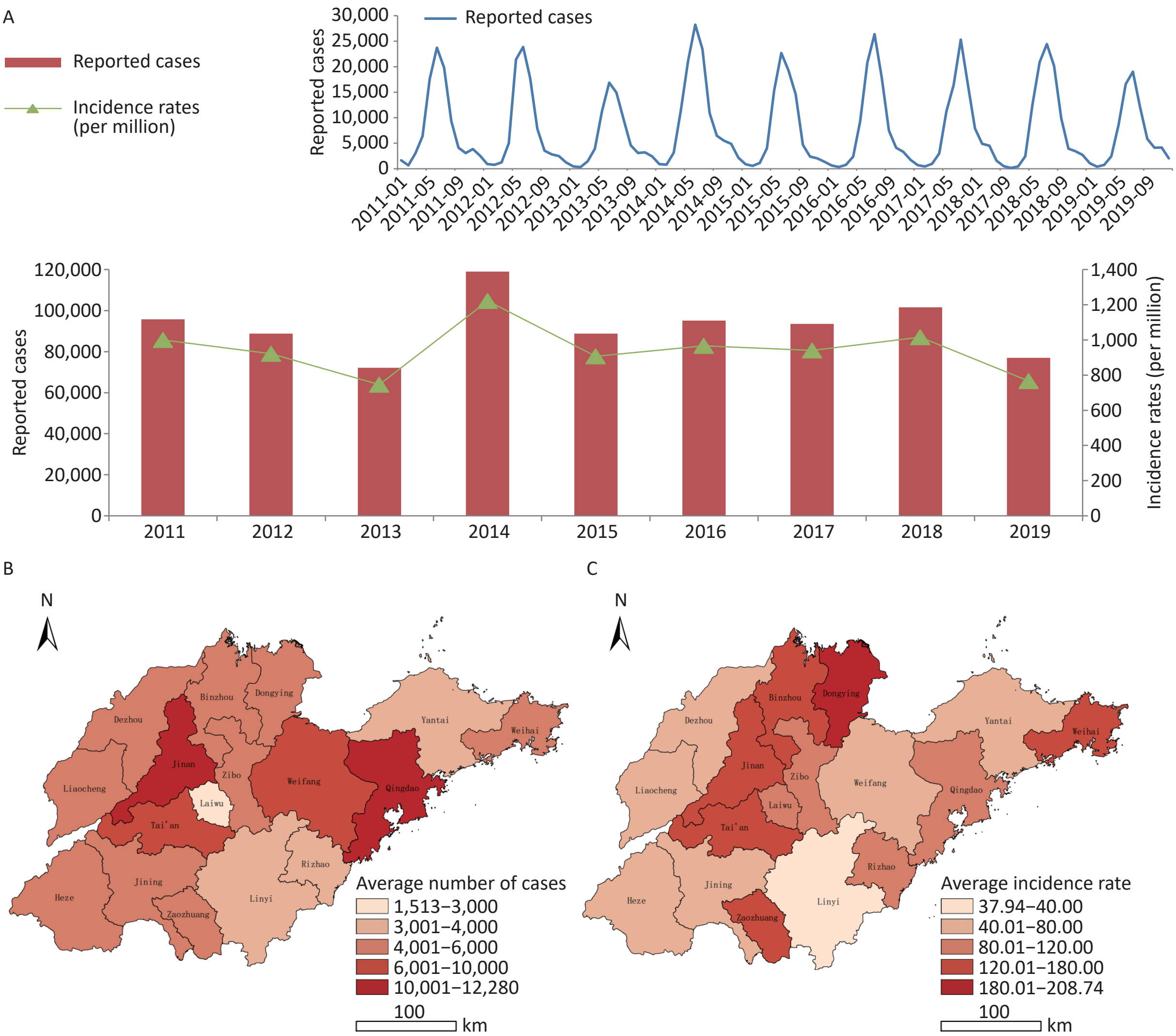

Supplementary Figure S4. (A) Epidemical curve of reported cases with HFMD between 2011 and 2019 in Shandong. (B) Geographic distribution of average number of probable and laboratory-confirmed cases. (C) Geographic distribution of average incidence rates of probable and laboratory-confirmed cases.

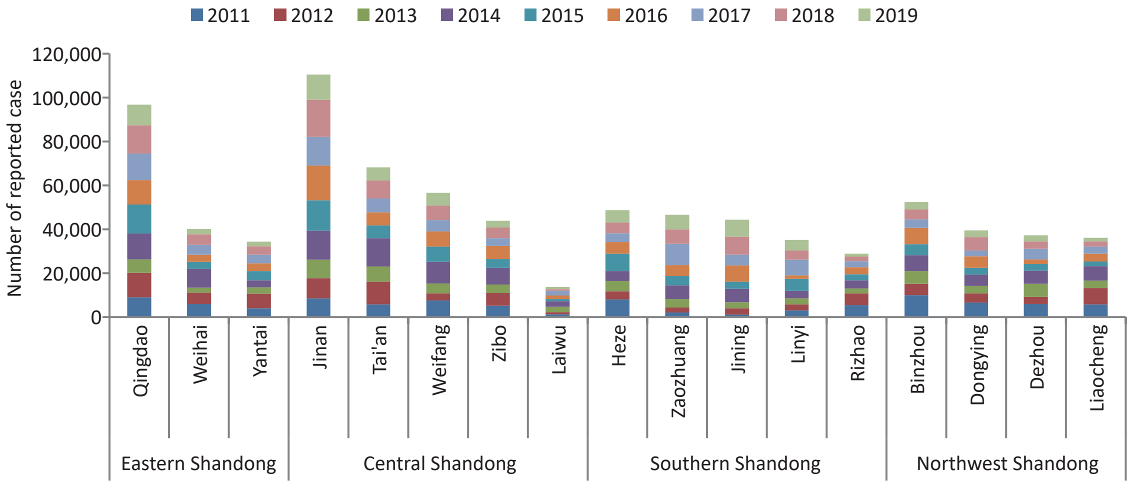

Supplementary Figure S5. Number of reported case of HFMD in cities of Shandong province between 2011 and 2019. Data was available from Chinese Disease Prevention and Control Information System (http://10.249.1.170:81).

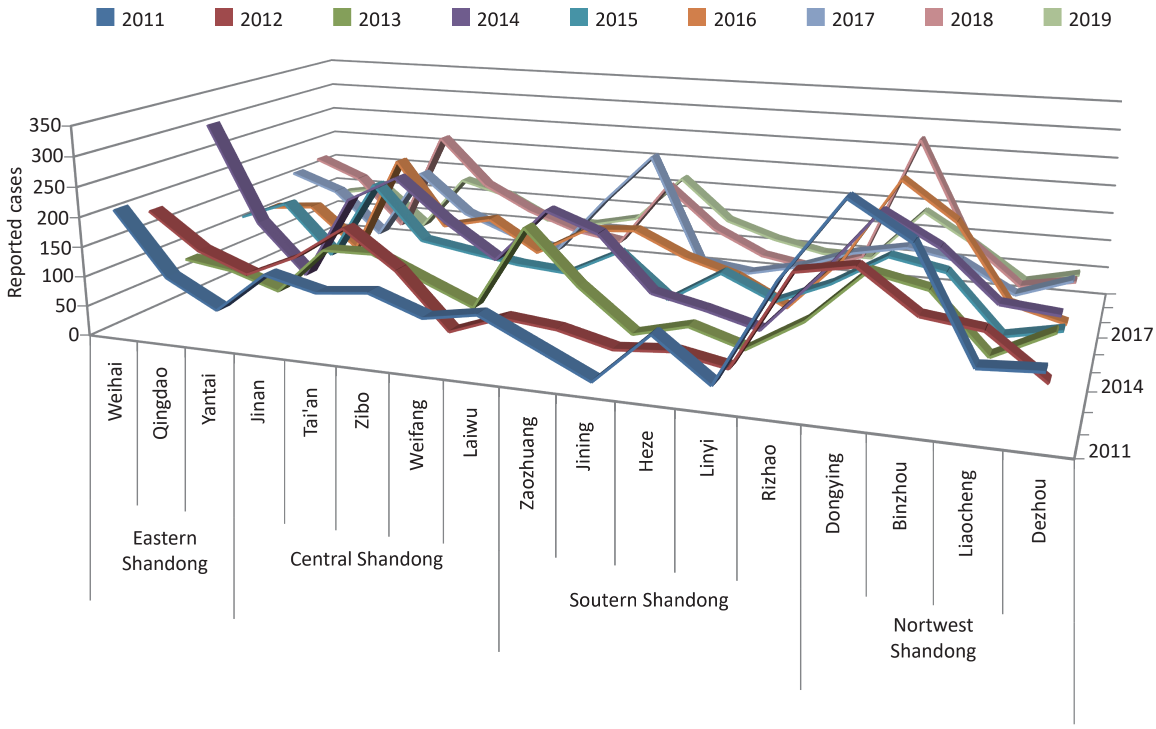

Supplementary Figure S6. Incidence of HFMD in cities of Shandong province between 2011 and 2019. Data was available from Chinese Disease Prevention and Control Information System (http://10.249.1.170:81).

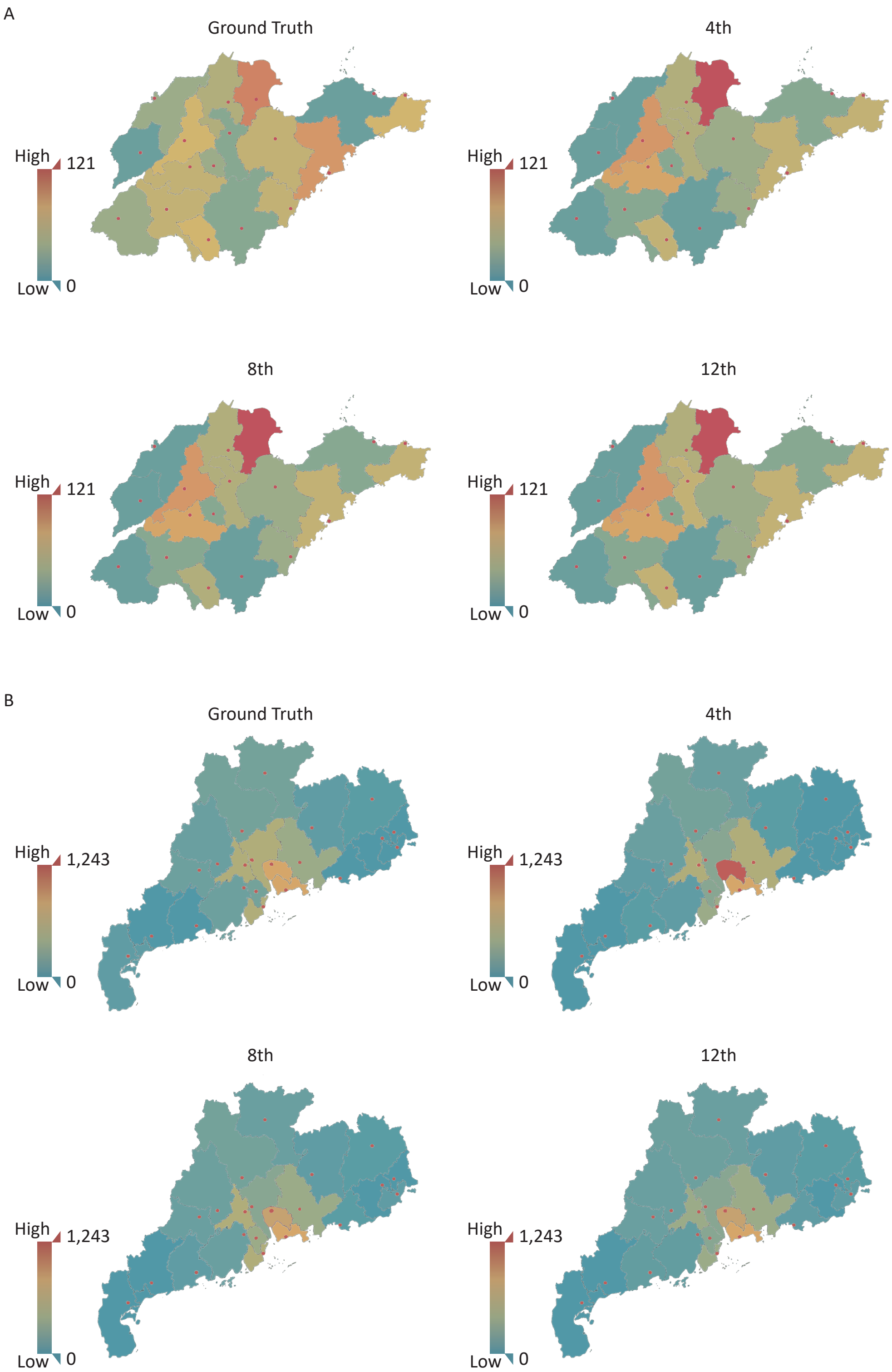

Supplementary Figure S7. The Geospatial map under different forecast lengths. (A) Geospatial map of Shandong Province on 29th week with the predicted length on 4 weeks, 8 weeks, and 12 weeks. (B) Geospatial map of Guangdong Province on 25th week with the predicted length on 4 weeks, 8 weeks, and 12 weeks.

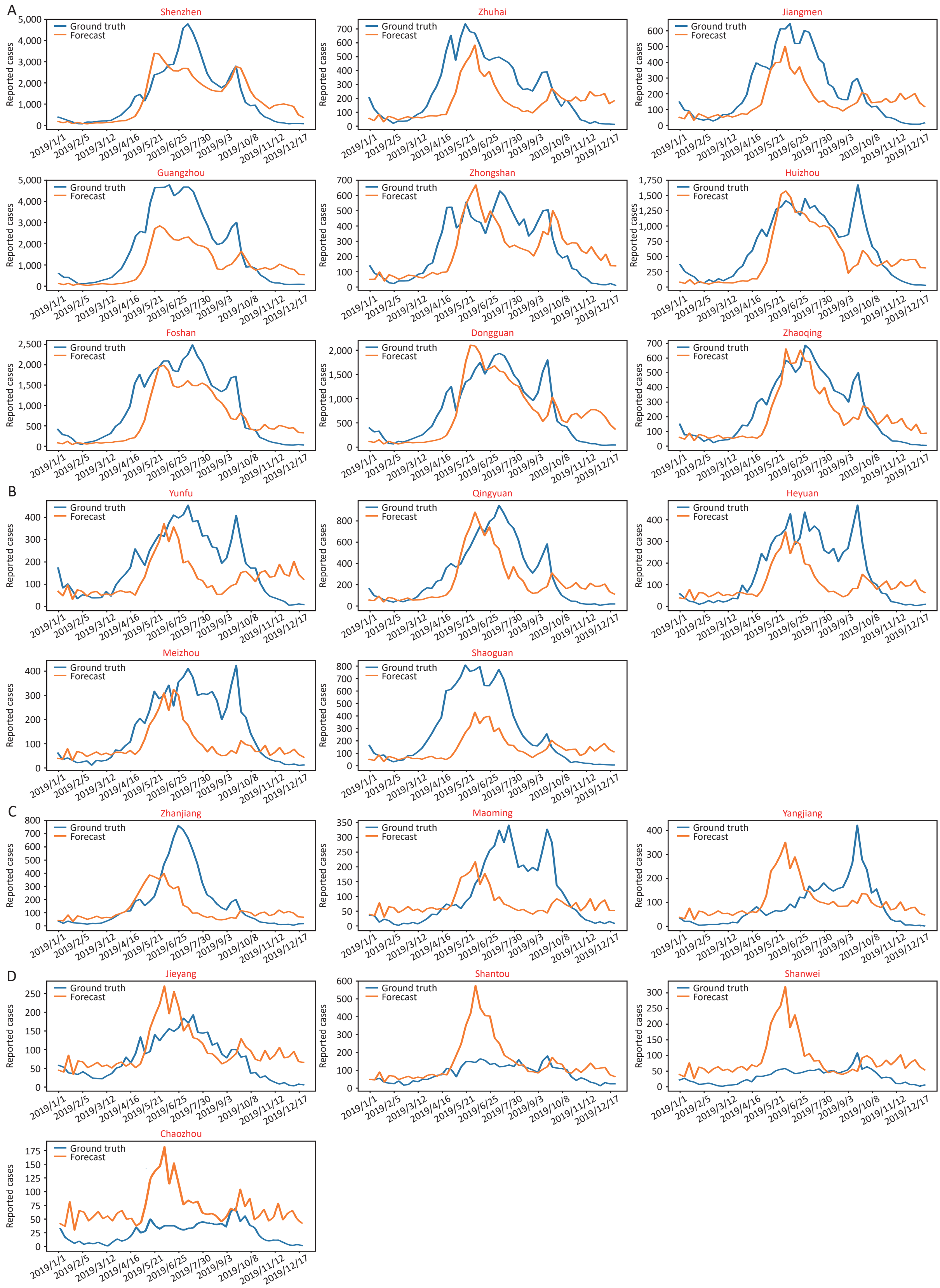

Supplementary Figure S8. The predictive epidemical curves about HFMD in Guangdong province, 2019. (A) Pearl River Delta region. (B) Eastern Guangdong. (C) Western Guangdong. (D) Northern Guangdong.

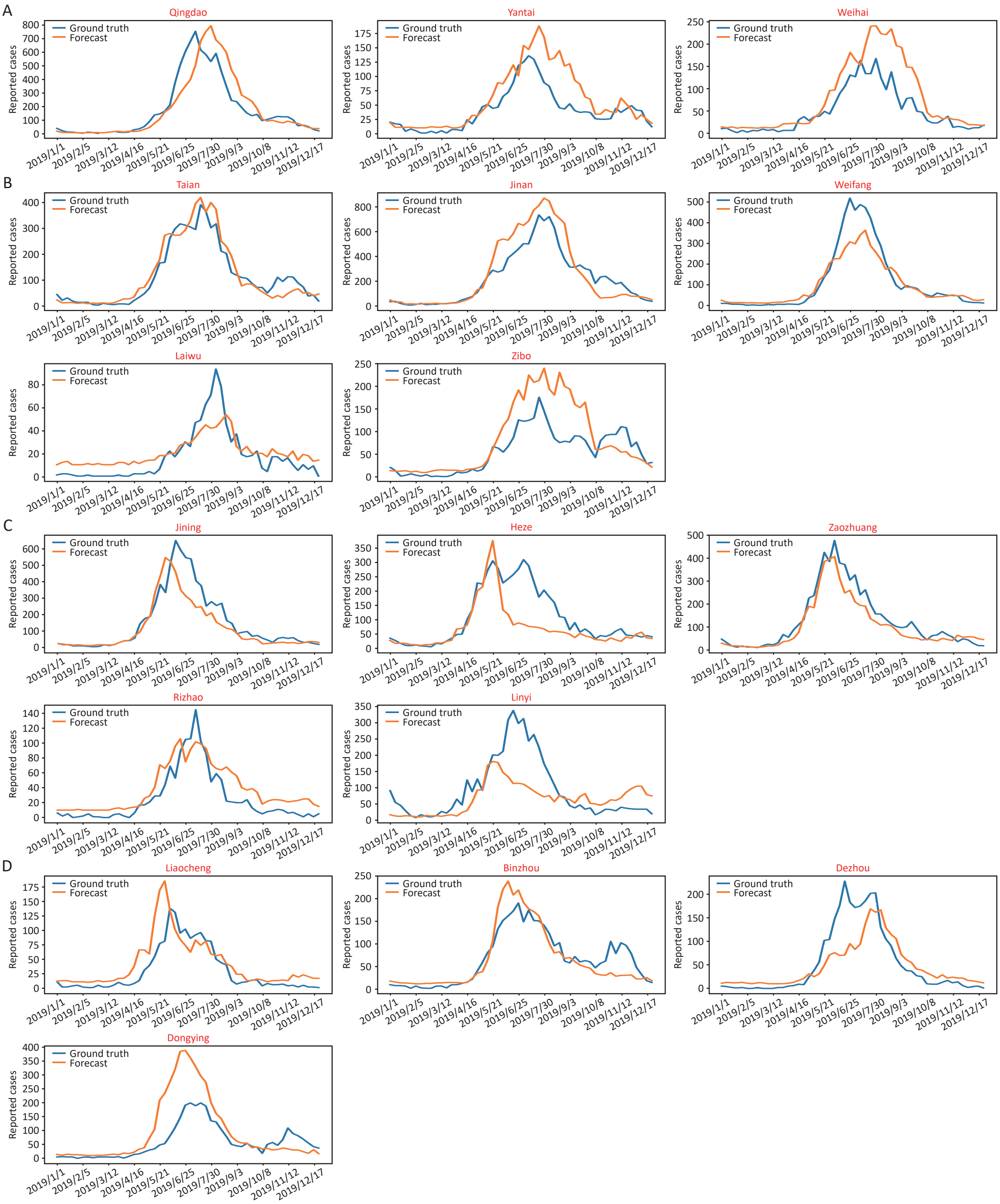

Supplementary Figure S9. The predictive epidemical curves about HFMD in Shandong province, 2019. (A) Eastern Shandong. (B) Central Shandong. (C) Southern Shandong. (D) Northwest Shandong.

Supplementary Table S1. The evaluation parameter with influence of historical data length

Province	**H**	**4 weeks**		**8 weeks**		**12 weeks**	
		MAE	RMSE	MAE	RMSE	MAE	RMSE
SD	12	57.47	96.41	50.71	83.95	41.09	68.81
	24	**35.49**	**62.17**	**35.46**	**62.18**	**36.08**	**62.19**
	36	41.60	75.89	44.98	79.99	45.78	74.17
GD	12	249.81	460.71	254.86	496.17	240.10	471.97
	24	215.51	449.10	**210.66**	**413.80**	**200.35**	**387.81**
	36	**210.21**	**408.58**	248.48	482.16	233.58	438.41

Supplementary Table S2. The evaluation parameter with influence of channel size

Province	**Channel size**	**4 weeks**		**8 weeks**		**12 weeks**	
		MAE	RMSE	MAE	RMSE	MAE	RMSE
SD	(1, 3, 5)	43.85	65.45	43.77	65.40	36.27	62.88
	(1, 4, 8)	**35.49**	**62.17**	**35.46**	**62.18**	**36.08**	**62.19**
	(1, 8, 16)	42.20	73.58	41.66	71.44	39.96	70.97
GD	(1, 3, 1)	215.51	449.10	**210.66**	**413.80**	**200.35**	**387.81**
	(1, 3, 6)	**188.67**	**328.90**	227.02	427.90	217.81	408.81
	(1, 3, 9)	190.18	386.10	226.38	420.60	225.80	432.63

Note. As two STblocks is mirrored, only channel parameters in the two convolution layers of the first STblock are shown in the table

Supplementary Table S3. The evaluation parameter with neighborhood number and time convolution kernel size in Shandong

Province	Convolution kernel size	Forecast weeks		Neighborhood number (ks)				
				1	2	3	4	5
SD	kt = 3	4	MAE	45.42	**35.49**	35.51	38.90	38.12
			RMSE	87.81	**62.17**	62.17	68.65	65.24
		8	MAE	42.46	**35.43**	51.27	40.49	38.48
			RMSE	75.96	**62.19**	95.13	70.05	64.93
		12	MAE	47.89	45.18	52.12	**41.48**	45.16
			RMSE	80.26	74.86	91.93	**71.29**	72.84
	kt = 5	4	MAE	40.57	40.76	40.92	**35.49**	37.59
			RMSE	75.16	71.27	75.45	**62.17**	64.45
		8	MAE	40.21	40.51	37.56	**35.46**	36.72
			RMSE	70.62	69.32	65.05	**62.18**	63.60
		12	MAE	42.07	45.81	46.41	**36.08**	41.97
			RMSE	73.55	66.58	74.01	**62.19**	72.15
GD	kt = 3	4	MAE	234.09	**211.31**	254.03	249.05	253.69
			RMSE	476.59	**407.89**	543.36	528.87	536.48
		8	MAE	247.83	**235.43**	253.99	254.03	253.88
			RMSE	477.57	**459.17**	535.11	543.39	535.53
		12	MAE	294.45	**226.98**	265.90	294.16	266.84
			RMSE	514.68	**450.50**	520.38	507.44	519.86
	kt = 5	4	MAE	255.34	256.64	216.56	294.07	**215.51**
			RMSE	547.23	549.49	482.12	527.87	**449.10**
		8	MAE	254.66	218.60	227.65	234.09	**210.66**
			RMSE	545.56	428.13	455.34	476.59	**413.80**
		12	MAE	263.03	245.47	256.89	215.43	**200.35**
			RMSE	522.21	471.83	528.53	435.24	**387.81**

Supplementary Table S4. The influence of graph convolution module in Shandong and Guangdong

Convolution kernel size	Forecast weeks		Shandong		Guangdong	
			With spatial	Without spatial	With spatial	Without spatial
kt = 3	4	MAE	**35.49**	44.95	**211.31**	214.43
		RMSE	**62.17**	82.34	**407.89**	457.11
	8	MAE	**35.43**	53.17	235.43	**231.67**
		RMSE	**62.19**	101.31	**459.17**	462.32
	12	MAE	**41.48**	43.96	**226.98**	232.07
		RMSE	**71.29**	77.46	**450.50**	452.03
kt = 5	4	MAE	**35.49**	45.85	215.51	**210.03**
		RMSE	**62.17**	66.61	449.10	**436.94**
	8	MAE	**35.46**	43.69	**210.66**	246.84
		RMSE	**62.18**	65.36	**413.80**	495.93
	12	MAE	**36.08**	45.77	**200.35**	225.48
		RMSE	**62.19**	66.56	**387.81**	427.83

Supplementary Table S5. The goodness of fit between the predicted curve and the actual incidence curve in Shandong

City	Predictive epidemical curve	R2	Average number of reported cases (2011–2018)	Average Morbidity (/million) (2011–2018)	City	Predictive epidemical curve	R2	Average number of reported cases (2011–2018)	Average Morbidity (/million) (2011–2018)
Laiwu	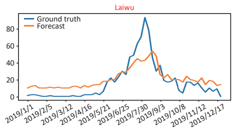	0.03	1,266.50	9.51	Binzhou	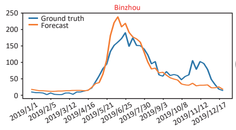	0.75	5,213.25	13.63
Linyi	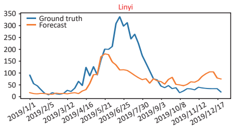	0.23	3,378.88	3.30	Qingdao	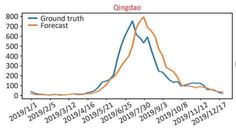	0.75	9,439.25	10.50
Heze	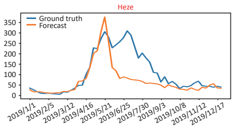	0.28	4,797.75	5.68	Weihai	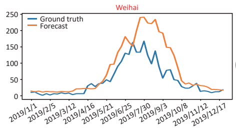	0.80	4465.22	13.03
Zibo	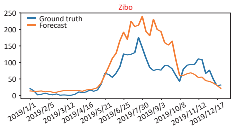	0.52	4,158.38	9.01	Jining	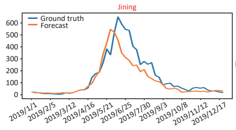	0.81	4920.22	5.97
Rizhao	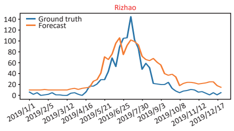	0.61	2,986.63	10.45	Jinan	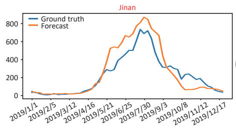	0.86	10,718.50	15.21
Dongying	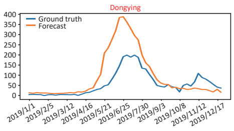	0.65	3,926.50	18.76	Tai.an	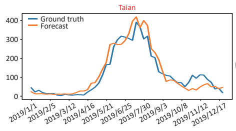	0.91	6,152.38	11.04
Liaocheng	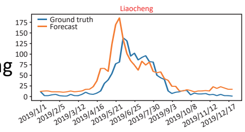	0.67	3,482.50	5.86	Weifang	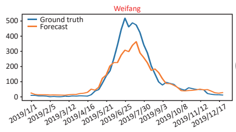	0.91	5,114.75	6.79
Dezhou	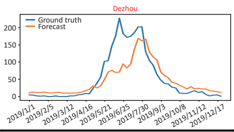	0.68	3,580.25	6.30	Zaozhuang	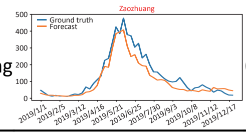	0.95	4,209.75	11.02

Supplementary Table S6. The goodness of fit between the predicted curve and the actual incidence curve in Guangdong

City	Predictive epidemical curve	R2	Average number of reported cases (2011–2018)	Average Morbidity (/million) (2011–2018)	City	Predictive epidemical curve	R2	Average number of reported cases (2011–2018)	Average Morbidity (/million) (2011–2018)
Yangjiang	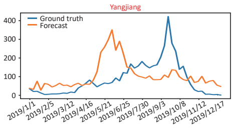	0.01	5402.88	17.69	Shaoguan	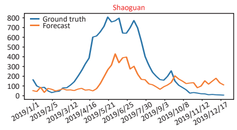	0.46	6432.63	22.14
Shanwei	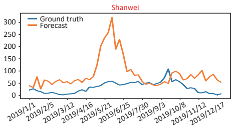	0.01	2932.38	9.81	Shenzhen	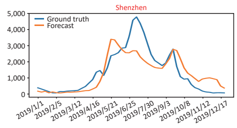	0.47	41759.13	37.67
Shantou	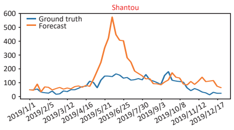	0.02	7168.88	12.82	Zhuhai	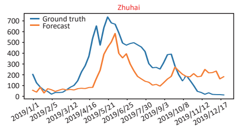	0.57	10453.00	64.52
Maoming	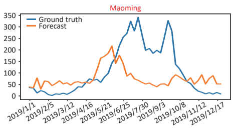	0.04	5157.50	8.64	Huizhou	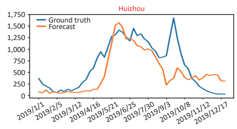	0.58	20951.63	44.79
Zhanjiang	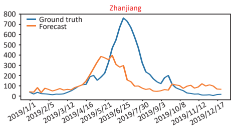	0.04	6609.50	9.27	Qingyuan	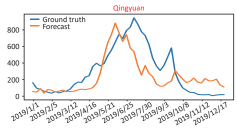	0.60	10853.75	34.64
Chaozhou	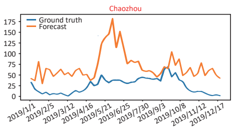	0.05	2588.88	9.66	Jiangmen	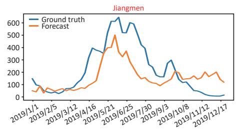	0.62	10017.25	28.21
Yunfu	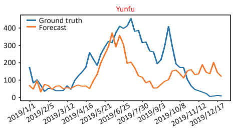	0.15	8478.38	34.90	Dongguan	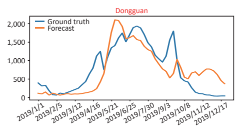	0.65	32108.13	38.71
Meizhou	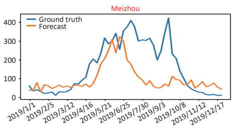	0.30	8592.13	19.88	Zhaoqing	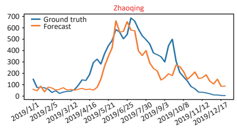	0.68	12463.63	30.97
Zhongshan	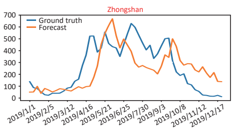	0.33	6609.50	44.10	Guangzhou	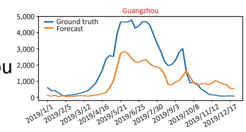	0.75	52876.38	39.84
Heyuan	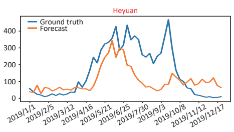	0.34	5519.38	22.11	Foshan	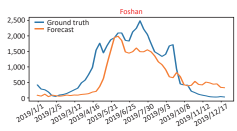	0.77	32410.25	44.00
Jieyang	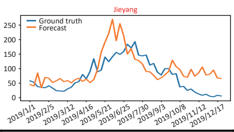	0.41	4335.00	7.22					